Available online at www.sciencedirect.com
SCIENCE DIRECT®
Journal of Catalysis 222 (2004) 348–356
JOURNAL OF CATALYSIS
www.elsevier.com/locate/jcat

Selective hydrogenation of α,β-unsaturated ketones to α,β-unsaturated alcohols on gold-supported catalysts

C. Milone,[a] R. Ingoglia,[a] A. Pistone,[a] G. Neri,[a] F. Frusteri,[b] and S. Galvagno [a,*]

[a] *Dipartimento di Chimica Industriale e Ingegneria dei Materiali, Università di Messina, Salita Sperone 31, I-98166 Messina, Italy*
[b] *Istituto CNR-TAE, Salita S. Lucia sopra Contesse 5, I-98126 Messina, Italy*

Received 8 August 2003; revised 5 November 2003; accepted 5 November 2003

Abstract

The liquid-phase reduction of α,β-unsaturated ketones [*trans*,4-phenyl,3-buten,2-one (benzalacetone $C_6H_5CH{=}CHCOCH_3$), 4-methyl,3-penten,2-one $(CH_3)_2C{=}CHCOCH_3$, and 3-penten,2-one $CH_3CH{=}CHCOCH_3$] to the corresponding α,β-unsaturated alcohols has been investigated on gold-supported catalysts. Au/Fe_2O_3 and Au/Al_2O_3 have been prepared by coprecipitation and deposition-precipitation. The catalytic behavior of a Au/Fe_2O_3 "reference" catalyst supplied by the World Gold Council has been also investigated. In the hydrogenation of benzalacetone and 4-methyl,3-penten,2-one on the "homemade" Au/Fe_2O_3 catalysts the unsaturated alcohol is the main reaction product. Chemoselectivity higher than 60% was achieved. On Au/Al_2O_3, the selectivity is 10%. It is noteworthy that within the gold supported on iron oxide samples, the reference catalyst shows the lowest selectivity toward the formation of the unsaturated alcohol. In the hydrogenation of 3-penten,-2-one on the homemade Au/Fe_2O_3, the saturated ketone is the main reaction product and the selectivity toward the formation of the unsaturated alcohol is 15% at conversion >90%. It is likely that the absence of bulky substituents on the conjugated C=C double bond favors its adsorption on the catalytic sites, leading to the formation of the saturated carbonyl compounds as the main reaction product. A detailed characterization of the investigated catalysts by TEM and XRD is also reported.

Keywords: Gold catalysts; Selective hydrogenation; α,β-Unsaturated ketones; α,β-Unsaturated alcohols

1. Introduction

The selective reduction of α,β-unsaturated ketones to α,β-unsaturated alcohols by molecular hydrogen has been attempted on heterogeneous catalysts for some time with very limited success [1,2].

A recent paper dealing with the selective hydrogenation of the C=O bond of a highly functionalized cyclic α,β-unsaturated ketone (ketoisophorone) reports selectivities to the unsaturated alcohol higher than 90% [3]. However, such appreciable results are obtained only in the hydrogenation of ketoisophorone. In the reduction of other substrates, having a sterically unhindered C=O group, the C=C double bond is preferentially hydrogenated.

The selective reduction of the conjugated C=O bond in a ketone can be easily achieved by using $LiAlH_4$ as reductant. Homogeneous catalysts such as phosphine-stabilized copper (I) hydride complexes are able to reduce the conjugated C=O double bond in the presence of molecular H_2 [4]. On heterogeneous catalysts the selective hydrogenation of the conjugated C=O bond is generally obtained by using isopropanol as a hydrogen source [5–8].

Gargano et al. have studied the chemoselective reduction of the *trans*,4-phenyl,3-buten,2-one (benzalacetone) and 5-hexen,2-one on metal oxides, via hydrogen transfer from isopropyl alcohol [5]. The allylic alcohols have been obtained with remarkable selectivity and yield. During the reduction of 5-hexen,2-one the selectivity toward the formation of the unsaturated alcohol was higher than 90% on CaO and La_2O_3, whereas in the hydrogenation of benzalacetone the chemoselectivity reached values higher than 80% on La_2O_3, Y_2O_3, and Al_2O_3.

Coman et al. [6] report that the reduction of a sterically hindered unsaturated ketone to a secondary allylic alcohol occurs with high yields on PtSn catalysts, in the presence of isopropanol as hydrogen donor. It has been suggested that the high chemoselectivity is favored by the low hydrogen

* Corresponding author.
E-mail address: galvagno@ingegneria.unime.it (S. Galvagno).

0021-9517/$ – see front matter
doi:10.1016/j.jcat.2003.11.003

coverage obtained by using isopropanol instead of H_2 and by the presence of bulky substituents on the C=C double bond which hinders its adsorption on the catalytic sites. The importance of a steric hindrance has been confirmed by experiments carried out with methyl vinyl ketone which, under similar reaction conditions, was mainly reduced to the saturated ketone [6]. It has also been proposed that the activation of the carbonyl group occurs on Sn^{n+} sites, in analogy with the widely accepted mechanism reported for the hydrogenation of α,β-unsaturated aldehydes [1,2,9].

In the present work we report the results of a study on the catalytic activity of gold-supported catalysts in the reduction of α,β-unsaturated ketones by dihydrogen. Preliminary results have already demonstrated that Au supported on Fe_2O_3 is able to hydrogenate the *trans*,4-phenyl,3-buten,2-one (benzalacetone) to the corresponding unsaturated alcohol with a selectivity higher than 60% at 90% of conversion [10].

It is known that gold catalysts are very selective in the hydrogenation of α,β-unsaturated aldehydes to the corresponding unsaturated alcohols in reactions occurring in either the gas phase on the liquid phase [11–13].

In this paper we will detail the study of the hydrogenation of benzalacetone on gold catalysts and we will also present the results obtained in the hydrogenation of other α,β-unsaturated ketones. Moreover, the catalytic behavior of "homemade" samples will be compared with a Au/Fe_2O_3 gold "reference" catalyst supplied by the World Gold Council.

2. Experimental

2.1. Sample preparations

Au-supported catalysts were prepared by coprecipitation and deposition-precipitation. The coprecipitation was carried out using $HAuCl_4$ (Fluka) and $Fe(NO_3)_3{\cdot}9H_2O$ (Fluka) as starting materials. An aqueous mixture of $HAuCl_4$ and $Fe(NO_3)_3{\cdot}9H_2O$ was poured into an aqueous solution of Na_2CO_3 1 M (pH 11.9) and kept at 353 K under vigorous stirring. The solids were digested overnight at room temperature and then washed with water until free of chloride ions ($AgNO_3$ test) and then dried under vacuum at 353 K for 1 day.

The deposition-precipitation of gold onto the supports was carried out in agreement with Haruta's procedure [14], by adding the support to an aqueous solution of $HAuCl_4$ previously adjusted at pH 7–8 with NaOH. The slurry was maintained at 343 K, under vigorous stirring, for 2 h. Then the samples were filtered, washed with deionized water until elimination of chloride, and then dried under vacuum at 353 K for 1 day.

Al_2O_3 support was a commercial product (Alpha Aesar purity 99.7%). Fe_2O_3 was prepared in agreement with the procedure used for the coprecipitation. The gold content of the catalysts was determined by measuring the adsorbance of gold solutions at $\lambda = 400$ nm [15]. The solutions were prepared by dissolving the catalysts in HCl–HNO_3 (3:1 by volume), and then adding a solution of tin(II) chloride in hydrochloric acid.

The reference catalyst, 4.4 wt% Au supported on Fe_2O_3, prepared by coprecipitation, was supplied by the World Gold Council.

The Ru/Fe_2O_3 sample (Ru nominal content = 2 wt%) was prepared by deposition of the metal colloid on the preformed support. The ruthenium nanoparticles were obtained by reduction of $RuCl_3$ in ethylene glycol following the procedure reported in Ref. [16]. Fe_2O_3 was then added to the colloidal solution under vigorous stirring to form a suspension. The catalysts was filtered, washed with water, and dried at 393 K for 2 h.

2.2. Sample characterization

Surface area measurements were made using the BET nitrogen adsorption method in a conventional volumetric apparatus, after outgassing (10^{-4} mbar) the sample at 353 K for 2 h.

XRD studies were carried out with an Ital-Structures diffractometer using nickel-filtered Cu$K\alpha$ radiation by mounting the powder samples on Plexiglas holders. Diffraction peaks were compared with those reported in the JCPDS Data File.

TEM analysis was performed on a Philips instrument Model CM12 operating at 120 kV and directly interfaced with a computer for real-time image processing. The catalyst specimens for electron microscopy were prepared by gently grinding the powder samples in an agate mortar, suspending, and sonicating them in isopropanol, and a drop of the suspension was placed on a carbon film copper grid. After evaporation of the solvent, the specimens were introduced into the microscope column. In order to obtain metal particles-size distribution, several hundred particles visible on the micrographs were counted.

The average value of the gold particle sizes was calculated by the following equation:

$$\bar{d} = \frac{\sum n_i d_i}{n_i}.$$

2.3. Catalytic activity

The catalytic experiments were carried out at atmospheric pressure under H_2 flow, at 333 K, in a 100-ml four-necked batch reactor fitted with a reflux condenser, dropping funnel, thermocouple, and magnetic stirrer head coupled with a gas stirrer (Model MRK 1/20-BR purchased by Premex Reactor). This gas stirrer was used to optimize the hydrogen transfer from the gas to the liquid phase. The catalyst (weight 0.5–1 g; particle size = 160–200 mesh) was added to 25 ml of solvent and treated at 343 K for 1 h under gaseous H_2.

The substrate (6×10^{-4} mol) was injected through one arm of the flask. The reaction mixture was stirred at 700 rpm.

The *trans*,4-phenyl,3-buten,2-one (benzalacetone) was supplied by ACROS, whereas the other reactants (4-methyl, 3-penten,2-one and 3-penten,2-one) were supplied by Fluka.

The progress of the reaction was followed by sampling a sufficient number of microsamples and analyzing them by means of GC-MS (Shimadzu GC-QP5000 Mod.). The reaction products were separated on a CP-WAX capillary column (1.20 µm, 60 m, 0.32 mm).

Catalytic activity was measured in terms of initial rates and calculated from the slope of the curves conversion versus time (t) at $t = 0$. Selectivities were calculated by the expression $S_i = C_i / \sum C_p$ where C_i is the concentration of product i and C_p the total concentration of the products. Preliminary tests carried out with different amounts of catalysts (0.2–1.0 g) grain size (80–200 mesh) and stirring rate (500–1000 rpm) indicated that under the conditions used the reaction is carried out in the absence of mass-transfer limitation.

3. Results and discussion

3.1. Chemical composition and surface area

Table 1 lists the chemical and morphological properties of the gold samples.

Catalysts prepared by coprecipitation have a gold loading ranging between 3 and 17 wt% and show an increase of the surface area with the gold content (entries 1–3). For sake of completeness the surface area of the reference catalyst has been measured under the same conditions as for the homemade solids and it is reported in Table 1. The lower BET surface area of the latter with respect to the analogous coprecipitated catalysts can be ascribed to calcination treatments to which the sample has been subjected. It should be noted that, unless otherwise specified, our samples were treated at 353 K.

Catalysts obtained by deposition-precipitation of the gold hydroxide onto preformed Al_2O_3 and Fe_2O_3 supports have a gold loading ranging between 2 and 6 wt% and BET surface area of about 120 m^2/g. Calcination in air of the AF5dp catalyst at 673 K for 2 h leads to a strong decrease of the surface area.

3.2. Transmission electron microscopy measurements

Representative TEM microphotographs of the "as prepared" coprecipitated and deposited-precipitated samples are shown in Figs. 1a and b. Different particles sizes and microstructures of the iron oxide support are obtained on the samples prepared with these two methods. On the AF16.6, prepared by coprecipitation, the support is in the form of aggregates of round nanometer particles of about 3–5 nm in diameter (Fig. 1a). No phase contrast characteristics of an amorphous material can be observed. On the AF5dp catalyst, the support exhibits a heterogeneous microstructure, likely due to the presence of different (crystalline) phases (Fig. 1b). On both catalysts, very large and irregular gold particles with low contrast have been observed, suggesting the presence of gold in an oxidized state.

TEM observations show that the morphological characteristics of the samples change after 1 h reduction in H_2, at 343 K in ethanol (Figs. 1c and d). In particular, small gold particles were clearly visible on the reduced catalysts. This may be due to the reduction of oxidized gold species to metallic gold and/or to the growth of native gold subnanometer particles favored by the H_2 flowing at 343 K, in ethanol. Moreover, on the coprecipitated catalysts the particles of support grew up to 7–10 nm in diameter (Fig. 1c).

The gold particle size distributions and the mean particle diameters of the reduced catalysts are reported in Fig. 2 and Table 1. On the coprecipitated catalyst AF3.1, the count of gold particles was very difficult, likely because of the low contrast with the support. Therefore, for this sample it was not possible to draw a true reliable distribution. Despite this limitation, TEM analysis clearly indicates that coprecip-

Table 1
Chemical composition, surface area (SA), mean gold particle size (nm), and catalytic activities (V_i) of gold-supported catalysts

Entry	Catalyst	Au (wt%)	Support	Preparation method	Mean gold particle size d (nm)	SA (m^2/g)	V_i[a] (10^7)
1	AF3.1	3.1	Fe_2O_3	Coprecipitation	–[c]	68	3.5 ± 0.2
2	AF5.3	5.3	Fe_2O_3	Coprecipitation	6.3	122	3.0 ± 0.2
3	AF16.6	16.6	Fe_2O_3	Coprecipitation	6.6	178	2.1 ± 0.1
4	AF5dp	5.4	Fe_2O_3	Deposition-precipitation	3.2	121	27.9 ± 1.4
5	AF5dp/c[b]	5.4	Fe_2O_3	Deposition-precipitation	39.4	34	< 0.1
6	Au/Fe_2O_3[d]	4.4	Fe_2O_3	Coprecipitation	2.8	39	1.1 ± 0.1
7	AAl2.3dp	2.3	Al_2O_3	Deposition-precipitation	4.3	124	1.0 ± 0.1

[a] V_i = initial rate of hydrogenation of benzalacetone (moles converted $g_{Au}^{-1}\,s^{-1}$).

[b] Calcined at 673 K for 2 h.

[c] Not determined due to the poor contrast with the support background.

[d] Gold "reference" catalyst, Type C, Lot No. Au/Fe_2O_3 02-3.

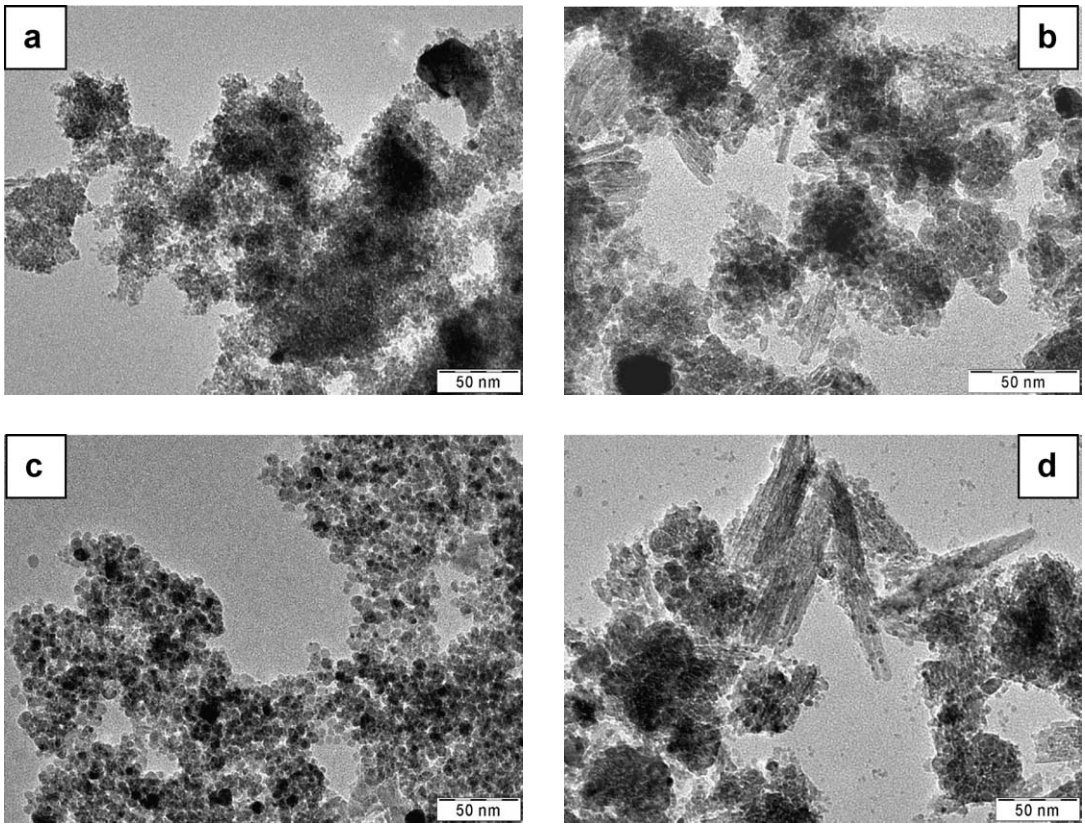

Fig. 1. TEM microphotographs of Au/Fe_2O_3 catalysts: (a) AF16.6 "as prepared," (b) AF5dp "as prepared," (c) AF16.6 reduced, (d) AF5dp reduced.

itated samples AF5.3 and AF16.6 have a larger particles size distribution than the AF5dp sample.

Fig. 3a shows the TEM microphotograph of the AF5dp calcined at 673 K for 2 h. A remarkable increase of the mean gold diameter was registered with respect to the uncalcined sample. On the calcined catalyst the majority of gold particles have a diameter between 10 and 80 nm. TEM microphotographs reported in Figs. 3b and c refer to the Au/Fe_2O_3 reference catalyst and the Au/Al_2O_3 sample, respectively. On the reference catalyst it can be clearly seen the plate-like morphology typical of well-crystallized hematite. On both catalysts small, well isolated, round and with good contrast gold crystallites having a narrow size distribution (Fig. 2) have been detected.

3.3. X-ray diffraction measurements

Structural characteristics of the catalysts have been investigated by X-ray diffraction (XRD). Fig. 4 shows the XRD of representative coprecipitated samples (patterns a–d). The as prepared catalysts (patterns a–c), dried at 353 K, show an almost amorphous feature regardless of the metal loading. These results are in agreement with our previous findings on similar catalysts [17] where it is reported that coprecipitated Au/Fe_2O_3 catalysts, with a gold loading higher than 1 wt%, show an amorphous feature, whereas at lower gold loading the support is better crystallized as hematite. This behavior has been ascribed to the retarding of the crystal growth of the iron phase by the presence of the gold ions. The diffraction peaks relative to metallic gold have never been detected.

After 1 h reduction in H_2, at 343 K, in ethanol, XRD patterns of the coprecipitated catalysts show some significant changes. As an example the XRD diffraction pattern of the reduced AF16.6 sample (pattern d) is reported. Reflections are attributed to magnetite (Fe_3O_4) coming from the low-temperature reduction of the amorphous iron(oxy-hydroxy) species which is catalyzed by the presence of gold. The reduction at low temperature of the iron oxide support has been previously evidenced by TPR experiments [15]. Moreover, the main diffraction peak of metallic gold at 38.1 (2θ) is noted.

Fig. 4 (pattern e) shows the XRD diffraction pattern of the reference catalyst. It shows a well-resolved reflection pattern attributed to hematite. This sample, obtained according to the coprecipitation method adopted by Haruta et al. [18], has been calcined during its preparation at high temperature and therefore the support is transformed into a crystalline phase.

X-ray diffraction patterns of the AF5dp and of the parent support are reported in Fig. 5 (patterns a and b). On the iron oxide the XRD analysis shows the presence of different crystalline iron oxy-hydroxides phases. Hematite (α-Fe_2O_3) is the prevailing crystallographic phase, but goethite (α-FeOOH) and ferrihydrite have also been found. Upon dispersing gold, through the deposition-precipitation

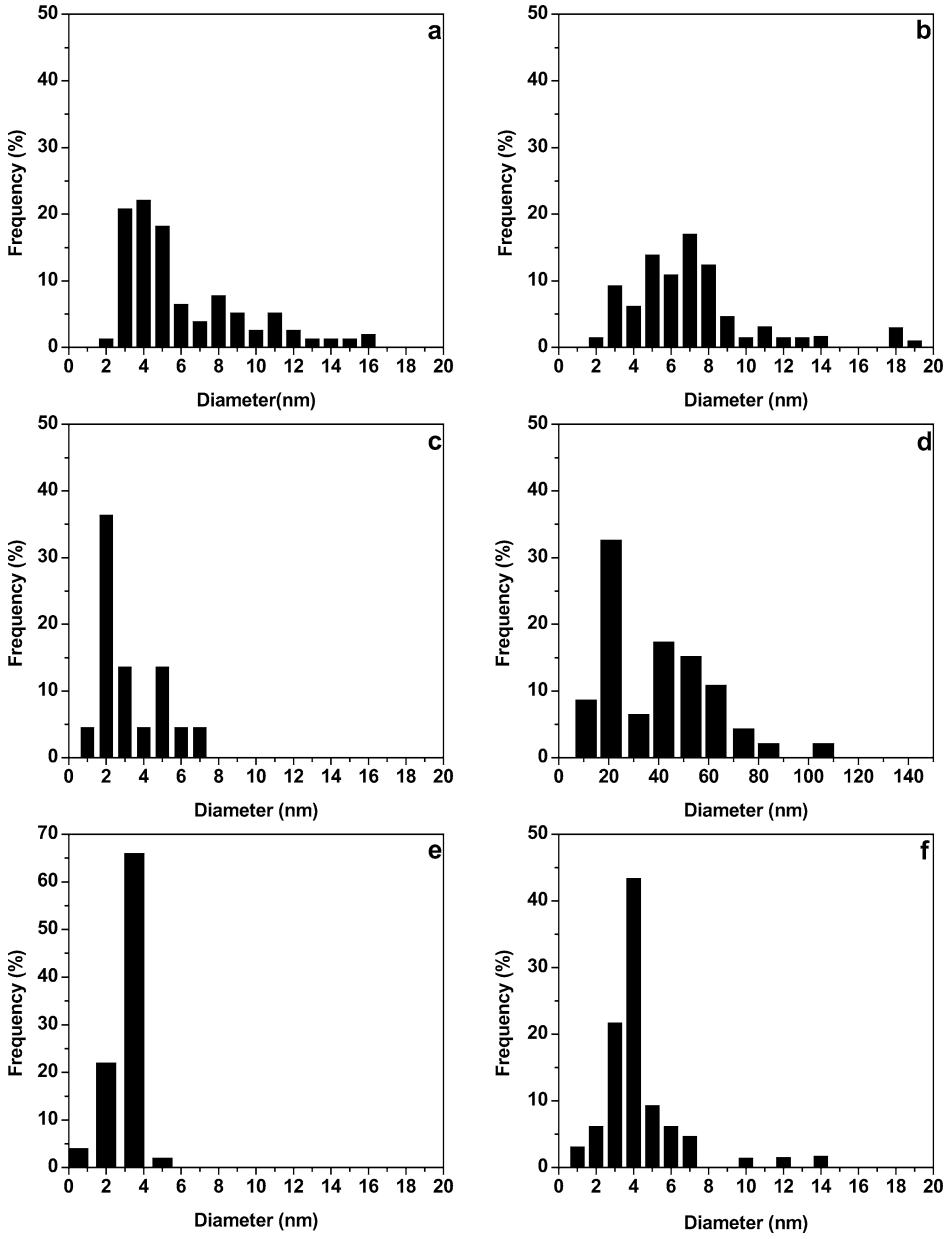

Fig. 2. Particle-size distribution of gold-supported catalysts: (a) AF5.3 reduced, (b) AF16.6 reduced, (c) AF5dp reduced, (d) AF5dp/c calcined at 673 K for 2 h, (e) Au/Fe_2O_3 reference, (f) AAl2.3dp reduced.

method, the ferrihydrite phase almost disappears. It is likely that during the deposition of gold, ferrihydrite is transformed into the more ordered hematite phase [19]. It is interesting to note that after 1 h reduction in H_2, at 343 K in ethanol, the XRD pattern of the AF5dp catalyst (pattern c) is substantially unmodified with respect to that of the as-prepared sample. This indicates the stability of the (crystalline) hematite phase under reducing conditions at low temperatures.

Calcination of AF5dp at 673 K for 2 h leads to the growth of the iron oxide particles, and consequently the intensity of the reflection peaks increases (Fig. 5, pattern f). The main crystallographic phase is hematite, whereas the diffraction peaks of goethite disappear. Moreover, the diffraction peaks of metallic gold are also observed.

3.4. Catalytic activity

Addition of H_2 to the unsaturated ketones can be described through the following simplified scheme where $R = H$, $R' = C_6H_5$ for benzalacetone, $R = H$, $R' = CH_3$ for 3-penten,2-one, and $R = CH_3$, $R' = CH_3$ for 4-methyl,3-penten,2-one.

Fig. 6 shows a typical course of the hydrogenation of benzalacetone on gold preparations.

In Table 1 is reported the rate of hydrogenation of benzalacetone ($C_6H_5CH{=}CHCOCH_3$) on gold preparations, expressed as initial rate of reaction per gram of metal.

It must be highlighted that the reduction of benzalacetone occurs by means of molecular H_2 and any mechanism

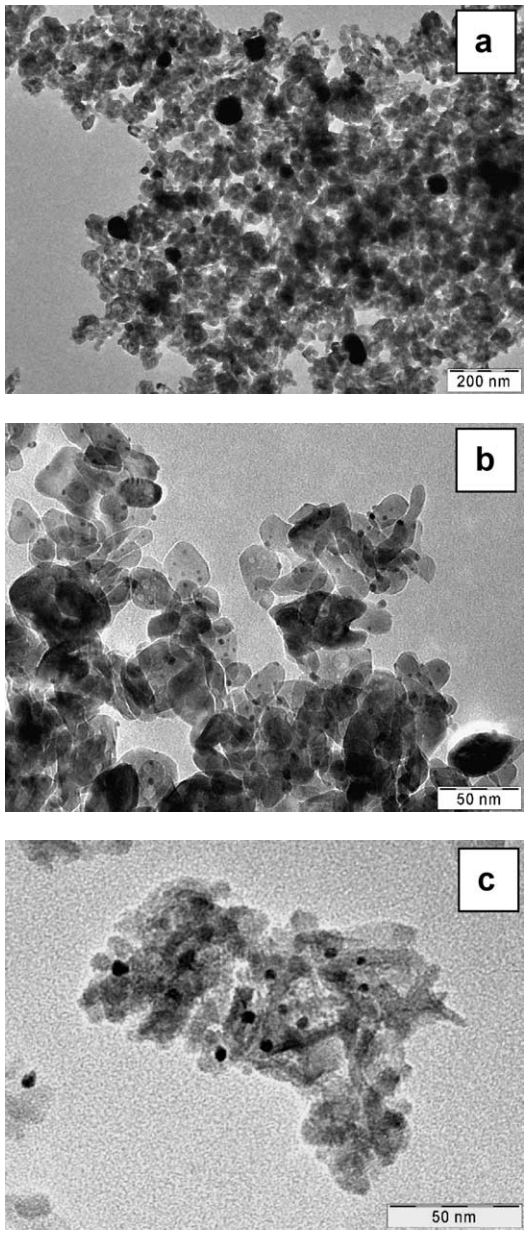

Fig. 3. TEM microphotographs of gold-supported catalysts: (a) AF5dp/c, calcined at 673 K for 2 h, (b) Au/Fe_2O_3 reference, (c) AAl2.3dp reduced.

involving the hydrogen transfer from the alcohol to the substrate was ruled out. This conclusion was drawn through a series of experiments carried out in the absence of hydrogen. As reported in Section 2, catalysts were prereduced in situ at 343 K for 1 h; the reactor was cooled down at the reaction temperature (333 K). In order to eliminate any residual H_2, the reactor was flushed with N_2. At this point the substrate was introduced into the reaction vessel. Under these conditions no conversion of benzalacetone was observed up to 3 h of contact time, thus indicating that the reducing agent is molecular H_2. Moreover, when H_2 was readmitted into the reactor, the hydrogenation of benzalacetone occurred.

Catalytic activity data of the homemade Au/Fe_2O_3 catalysts (Table 1) clearly show that the rate of reaction is

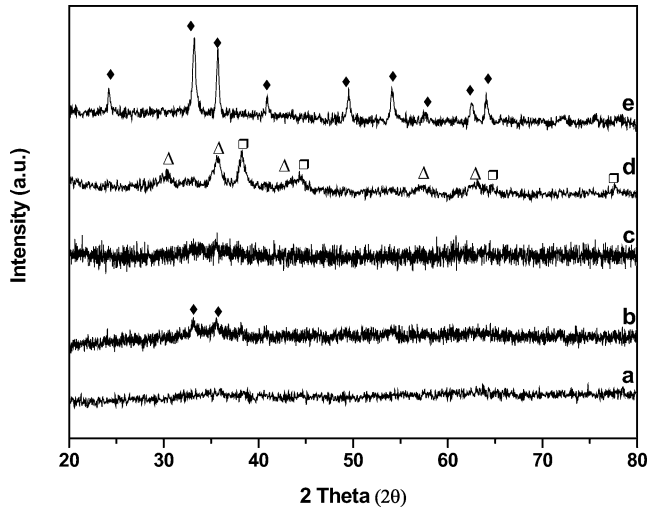

Fig. 4. XRD spectra of catalysts prepared by coprecipitation: (a) AF3.1, (b) AF 5.3, (c) AF16.6, (d) AF16.6 reduced, (e) Au/Fe_2O_3 reference. (◆) hematite; (□) metallic gold; (△) magnetite.

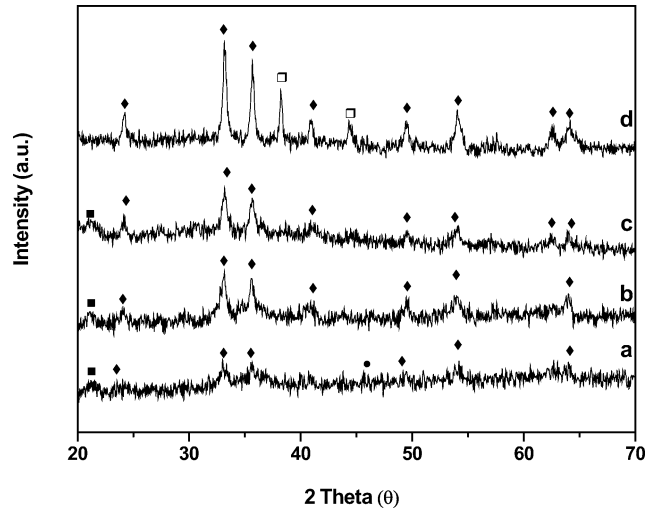

Fig. 5. XRD spectra of catalysts prepared by deposition-precipitation: (a) Fe_2O_3, (b) AF5dp, (c) AF5dp reduced, (d) AF5dp/c calcined at 673 K for 2 h. (◆) hematite; (□) metallic gold; (■) goethite; (●) ferrihydrite.

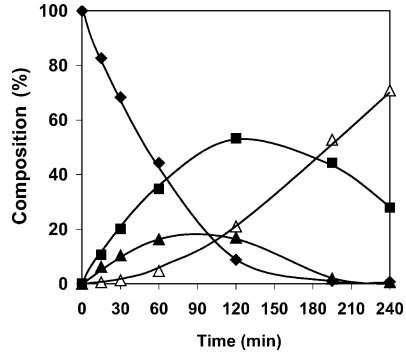

Fig. 6. Typical reaction course during the hydrogenation of benzalacetone on the "homemade" Au/Fe_2O_3 catalysts. (Reaction conditions: $T = 333$ K, $P_{H_2} = 1$ atm, ethanol = 25 ml, benzalacetone $= 6 \times 10^{-4}$ mol, AF5dp catalyst = 0.500 g.) Benzalacetone (◆), saturated ketone (▲), unsaturated alcohol (■), saturated alcohol (△).

strongly influenced by the preparation method. Catalyst prepared by coprecipitation (entry 2) is much less active than a analogous sample prepared by deposition-precipitation (entry 4). Within the same preparation method, instead, the catalytic activity decreases with increasing gold content (entries 1–3).

The higher catalytic activity of the sample prepared by deposition-precipitation, AF5dp, with respect to the AF5.3 sample could be due to the higher dispersion of gold (Table 1) and/or to a higher amount of gold exposed on the external surface of the support. It is well known that in solids prepared by coprecipitation and dried at 353 K, gold is mainly buried into the iron oxy-hydroxide matrix [20], whereas a higher amount of exposed gold is obtained through the deposition-precipitation method [21].

The Au/Fe_2O_3 reference catalyst shows a lower catalytic activity with respect to the homemade iron oxide-supported catalysts. This low activity is likely related to the calcination procedure used in the preparation of the reference sample to obtain metallic gold. Calcination of the solid is, in fact, detrimental for the catalytic activity. As it is shown in Table 1, the hydrogenation rate of the AF5dp/c (calcined at 673 K) dramatically decreases with respect to that of the as-prepared catalyst.

From the data reported in Table 1 no definitive conclusion on the effect of gold particle size on the rate of reaction can be drawn. On the three samples prepared by the same coprecipitation method, the decrease of activity can be simply due to a decrease of the gold surface area.

The formation of the unsaturated alcohol has been observed on all gold supported catalysts and the selectivity measured at low and high conversion are reported in Table 2.

Table 2
Catalytic activity and selectivity toward the formation of the unsaturated alcohol in the hydrogenation of benzalacetone

Catalyst	Au	Conversion	Selectivity (%)		
	(wt%)	(%)	SK	UA	SA
AF3.1	3.1	23.9	42.4	**51.8**	5.8
		95.1	1.4	**57.0**	41.6
AF5.3	5.3	21.6	35.8	**57.3**	6.9
		95.1	1.5	**56.2**	42.3
AF16.6	16.6	20.4	28.4	**64.2**	7.4
		90.4	11.2	**67.5**	21.2
AF5dp	5.4	17.3	35.8	**61.3**	2.9
		91.2	18.6	**58.5**	23.0
Au/Fe_2O_3[a]	4.4	17.6	77.9	**20.4**	1.7
		84.0	77.3	**19.8**	1.9
AF5dp/c	5.4	11.0	100	–	–
AAl2.3dp	2.3	21.9	85.1	**11.4**	3.5

SK, saturated ketone; UA, unsaturated alcohol; SA, saturated alcohol.
[a] Gold reference catalyst, Type C, Lot No. Au/Fe_2O_3 02-3.

It can be noted that the selectivity to the unsaturated alcohol (UA) remains almost constant regardless of the level of conversion whereas the selectivity to the saturated alcohol (SA) increases as that of the saturated ketone decreases (SK). This indicates that the formation of the saturated ketone and of the unsaturated alcohol occurs through parallel reactions, whereas the saturated alcohol is mainly obtained by the further hydrogenation of the C=O bond of the saturated ketone (Scheme 1).

All the homemade Au/Fe_2O_3 preparations, but AF5dp/c, show a remarkable selectivity toward the hydrogenation of the C=O bond in the whole range of conversion investigated.

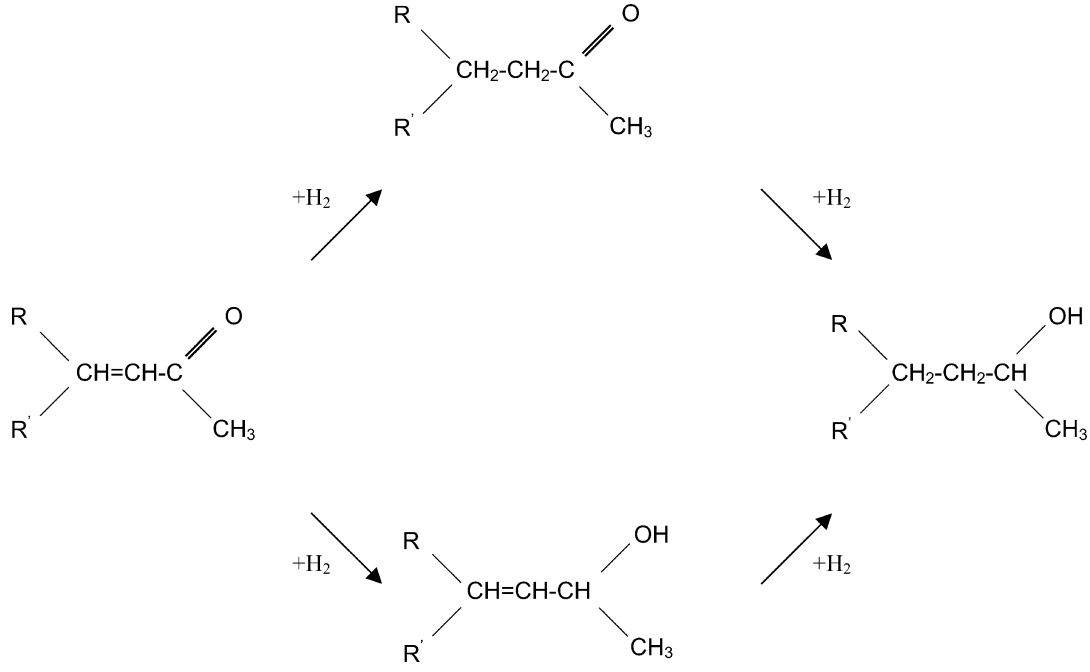

Scheme 1.

Table 3
Catalytic activity and selectivity toward the formation of unsaturated alcohol in the hydrogenation of α,β-unsaturated ketones

Substrate	Catalyst	Conversion	Selectivity (%)		
		(%)	SK	UA	SA
Benzalacetone	AF5dp	17.3	35.8	**61.3**	2.9
		91.2	18.6	**58.5**	23.0
4-methyl,3-penten,2-one	AF5dp	22.1	34.6	**60.7**	4.7
		89.1	9.8	**64.9**	12.3
3-penten,2-one	AF5dp	20.3	83.3	**14.3**	2.4
		90.2	59.8	**16.2**	24.0

SK, saturated ketone; UA, unsaturated alcohol; SA, saturated alcohol.

We have also studied the hydrogenation of 4-methyl,3-penten,2-one [$(CH_3)_2C{=}CHCOCH_3$] and of 3-penten,2-one [$CH_3CH{=}CHCOCH_3$]. The product distribution, at low and high conversion, is reported in Table 3. It can be seen that Au/Fe_2O_3 catalysts are able to hydrogenate selectively the conjugated C=O bond on substrates having a sterically unhindered C=O bond with respect to benzalacetone. The replacement of the bulky phenyl group of benzalacetone with two methyl groups on the C=C bond in the 4-methyl,3-penten,2-one does not lead to substantial differences in the product distribution. The α,β-unsaturated alcohol remains the main reaction product with a selectivity higher than 60% in the whole range of conversion investigated. In the hydrogenation of the 3-penten,2-one, which has only one methyl group as a substituent on the C=C bond, the selectivity toward the formation of the unsaturated alcohol drops to almost 15%. In analogy with the behavior observed in the hydrogenation of the α,β-unsaturated aldehydes, the presence of less bulky substituents on the conjugated C=C bond favors its adsorption on the catalytic sites leading to the preferential formation of the saturated carbonyl compound [1,22].

In the hydrogenation of benzalacetone on the homemade Au/Fe_2O_3 catalysts prepared by coprecipitation (Table 2), the selectivity toward the hydrogenation of the C=O group increases slightly with gold loading. Au/Fe_2O_3 prepared by deposition-precipitation shows a slight higher selectivity than analogous sample prepared by coprecipitation (Table 2). Within the gold supported on iron oxide catalysts, the reference sample shows the lowest selectivity toward the formation of the unsaturated alcohol.

Claus et al. [11] in their investigation of the hydrogenation of acrolein on Au-supported catalysts have reported that the selectivity toward the formation of the unsaturated alcohols increases with increasing particle size in the range 1–5 nm. They speculate that the adsorption of the C=O group of the α,β-unsaturated aldehyde is favored by face atoms, whereas sites with low coordination strongly favor the activation of the C=C bond. A similar correlation has also been found by Hutchings and co-workers [12] in their work on the hydrogenation of buten-2-al on Au/ZnO catalysts.

In our case, it seems that the selectivity to the unsaturated alcohol cannot be univocally correlated to the gold particle sizes. If we compare the results obtained on the AF5dp and AF5.3 catalysts, we could conclude that the dimensions of the metal particles do not influence the selectivity. Indeed, the selectivity of the two samples toward the hydrogenation of the conjugated C=O bond is quite similar (Table 2), notwithstanding the difference in the mean gold particles size (Table 1). However a small increase in selectivity is observed on the AF16.6 sample having larger gold particles (Table 1) and prepared similarly to the AF5.3 sample. A more detailed investigation on the effect of the metal particle size is necessary to elucidate this effect on the selective hydrogenation of unsaturated ketones.

It should also be noted that the chemical nature of the support strongly influences the activation of the conjugated C=O bond. Among the uncalcined samples, gold supported on Al_2O_3 shows the lowest selectivity toward the formation of the unsaturated alcohol, indicating that iron oxide promotes the hydrogenation of the C=O bond with an increase of the selectivity toward the formation of the unsaturated alcohol (Table 2).

Calcination of the AF5dp sample at 673 K decreases strongly the catalytic activity. On this calcined sample the only reaction product was the saturated ketone (Tables 1 and 2). A lower selectivity has also been measured on the reference sample, likely due to the calcination treatment used to obtain metallic gold. From the XRD characterization it seems that the promotion effect is caused by poor crystallized oxy-hydroxide phases. When all the iron is in the form of well-crystallized hematite the catalytic activity and selectivity drop drastically.

It should be highlighted that the presence of iron oxide is not sufficient to enhance the hydrogenation rate of the C=O with respect to the C=C bond in the hydrogenation of the α,β-unsaturated ketones, but it is necessary to have both gold and iron oxides. This indicates that the catalytic behavior arises from a synergetic effect between the two constituents. Indeed, when the hydrogenation of benzalacetone is carried out on Ru supported on Fe_2O_3, prepared dispersing colloids of ruthenium on the preformed Fe_2O_3 (see Section 2), the main reaction product is the saturated ketone and the selectivity toward the formation of the unsaturated alcohol is less than 2%. For sake of completeness, it must be noted that the Ru/Fe_2O_3 has been reduced under the same conditions as gold preparation (1 h in H_2, at 343 K, in ethanol). The XRD diffraction pattern of the reduced Ru/Fe_2O_3 is similar to that of the parent support (Fig. 5a). Therefore in the Ru/Fe_2O_3 the iron oxide is mainly presents as poorly crystallized oxy-hydroxide phase, which is suitable to promote the C=O hydrogenation on the gold catalysts.

In order to gain more information on this point we have also studied the hydrogenation of cinnamaldehyde (*trans*,3-phenyl,2-propen,1-al $C_6H_5CH{=}CHCHO$) the α,β-unsaturated aldehyde corresponding to benzalacetone. Table 4 reports the product distribution obtained in the hydrogenation of the cinnamaldehyde on the different catalysts. Au/Fe_2O_3 are the most selective samples regardless of gold

Table 4
Selectivity toward the formation of α,β-unsaturated alcohol in the hydrogenation of cinnamaldehyde

Catalyst	Me	Conversion	Selectivity (%)		
	(wt%)	(%)	SAL	UA	SAC
AF5.3	5.3	50.2	13.6	**83.8**	2.6
AF5dp	5.4	56.3	3.3	**86.9**	9.8
Au/Fe_2O_3[a]	4.4	48.2	25.3	**73.2**	1.6
AAl2.3dp	2.3	50.1	33.9	**60.3**	5.8
Ru/Fe_2O_3	2	50.3	8.1	**74.9**	17.0
Ru/Al_2O_3	2	51.2	80.7	**10.2**	9.1

Reaction conditions: $T = 333$ K, $P_{H_2} = 1$ atm, ethanol = 25 ml, cinnamaldehyde $= 6 \times 10^{-4}$ mol, catalyst weight = 0.500 g. SAL, saturated aldehyde; UA, unsaturated alcohol; SAC, saturated alcohol.
[a] Gold "reference" catalyst, Type C, Lot No. Au/Fe_2O_3 02-3.

loading and preparation method, in agreement with our previous findings [13]. It is noteworthy that an enhancement of the selectivity is also obtained when Ru is dispersed on Fe_2O_3. This Ru sample is totally unselective in the hydrogenation of benzalacetone.

To explain the promoting effect of iron it has been previously suggested that it acts as a Lewis acid which increases the polarization of the C=O bond facilitating the attack of the weak nucleophilic hydrogen adsorbed on the metal sites [9,13].

The promoting effect of the Lewis acid, however, is not always operating. In the hydrogenation of the α,β-unsaturated aldehydes it is known that when palladium is used as catalyst only the corresponding saturated aldehyde is formed, regardless of the presence of a promoter. On the other hand, when α,β-unsaturated ketones are hydrogenated the promoter has no effect on the selectivity on all but the Au metal catalysts.

The reason why palladium is so selective toward the formation of the saturated aldehydes has been attributed to the preferential adsorption of the conjugated system as a 1,4-C=C–C=O species. The hydrogenation of such a species would result in the formation of an unstable enol intermediate which will isomerize rapidly to the saturated aldehyde. Therefore no effect of promoter on the selective hydrogenation of the C=O bond can be observed [23]. On these bases it could be suggested that, when a substituent is added to the C=O group (ketone) the direct adsorption through the carbonylic function (1,2-C=O adsorbed species) is hindered and therefore the 1,4-C=C–C=O mode will be the preferential adsorption. As suggested for palladium, this species can lead only to the saturated ketone and therefore no effect of the promoter can be observed. Opposite to palladium, gold is likely a metal on which the 1,4-C=C–C=O adsorption mode is not favored and therefore the 1,2-C=O adsorbed species is formed also in the case of ketones. The scarce abundance of the 1,4-C=C–C=O species on gold catalysts is in agreement with the higher intrinsic selectivity observed also in the hydrogenation of unsaturated aldehydes in the absence of promoter [11–13].

4. Conclusions

From the results reported in this paper, the following main conclusions can be drawn: (a) gold is an intrinsically selective catalyst for the hydrogenation of the C=O bond; (b) iron oxide favors the activation of the C=O bond; (c) the promoting effect of iron oxide depends strongly on the substrate and on the catalytically active metal. No clear effect of the gold particle size on the catalytic activity and selectivity has been observed. Calcination of the iron oxide decreases the catalytic activity and selectivity. From the characterization results it is not possible to identify definitely the nature of the iron sites responsible for C=O activation.

Acknowledgment

This work was performed with the financial support of Ministero dell'Istruzione, Università e Ricerca (MIUR) through a COFIN 2001 grant.

References

[1] V. Ponec, Appl. Catal. A: Chem. 149 (1997) 27.
[2] R.L. Augustine, Catal. Today 37 (1997) 419.
[3] M. von Arx, T. Mallat, A. Baiker, J. Mol. Catal. A: Chem. 148 (1999) 275.
[4] J.-X. Chen, J.F. Daeuble, D.M. Brestensky, J.M. Stryker, Tetrahedron 56 (2000) 2153.
[5] M. Gargano, V. D'Orazio, N. Ravasio, M. Rossi, J. Mol. Catal. 58 (1990) L5.
[6] S.N. Coman, V.I. Parvulescu, M. De Bruyn, D.E. De Vos, P. Jacobs, J. Catal. 206 (2002) 218.
[7] A.J. Blacker, S.M. Brown, C. Bubert, J.M.J. Williams, WO 0244111 (2002).
[8] A.J. Blacker, B.V. Mellor, US patent 2002/0156282 (2002).
[9] Z. Poltarzewki, S. Galvagno, R. PietroPaolo, P. Staiti, J. Catal. 102 (1986) 190.
[10] C. Milone, R. Ingoglia, M.L. Tropeano, G. Neri, S. Galvagno, Chem. Commun. (2003) 868.
[11] P. Claus, A. Brückner, C. Mohr, H. Hofmeister, J. Am. Chem. Soc. 122 (2000) 11430.
[12] J.E. Bailie, H.A. Abdullah, G.J. Hutchings, et al., Phys. Chem. Chem. Phys. 3 (2001) 4113.
[13] C. Milone, M.L. Tropeano, G. Gulino, G. Neri, R. Ingoglia, S. Galvagno, Chem. Commun. (2002) 868.
[14] M. Haruta, Catal. Technol. 6 (3) (2002) 102.
[15] F.E. Beamish, J.C. van Loon, in: Analysis of Noble Metals, Academic Press, New York, 1977.
[16] A. Miyazaki, I. Balint, K.-i. Aika, Y. Nakano, J. Catal. 204 (2001) 364.
[17] G. Neri, A.M. Visco, S. Galvagno, M. Panzalorto, Thermochim. Acta 329 (1999) 39.
[18] M. Haruta, S. Tsubota, T. Kobayashi, H. Kageyama, M. Genet, B. Delmon, J. Catal. 144 (1993) 175.
[19] U. Schewertmann, R.M. Cornell, in: Iron Oxides in the Laboratory: Preparation and Characterization, VCH, Weinheim, 1991.
[20] M. Haruta, H. Kageyama, N. Kamijo, T. Kobayashi, F. Delannay, Stud. Surf. Sci. 44 (1988) 33.
[21] S. Scirè, S. Minicò, C. Crisafulli, C. Satriano, A. Pistone, Appl. Catal. B 40 (2003) 43.
[22] P. Gallezot, D. Richard, Catal. Rev.-Sci. Eng. 40 (1&2) (1998) 81.
[23] F. Delbecq, P. Sautet, J. Catal. 152 (1995) 217.